

# Novel antibiotics: C-2 symmetrical macrocycles inhibiting Holliday junction DNA binding by *E. coli* RuvC

Po-Shen Pan,<sup>a,†</sup> Fiona A. Curtis,<sup>b,†</sup> Chris L. Carroll,<sup>a</sup> Irene Medina,<sup>a</sup>  
Lisa A. Liotta,<sup>a</sup> Gary J. Sharples<sup>b,\*</sup> and Shelli R. McAlpine<sup>a,\*</sup>

<sup>a</sup>Department of Chemistry and Biochemistry, San Diego State University, 5500 Campanile Drive, San Diego, CA 92182-1030, USA

<sup>b</sup>Centre for Infectious Diseases, Wolfson Research Institute, University of Durham, Queen's Campus, Stockton-on-Tees TS17 6BH, UK

Received 28 February 2006; revised 10 March 2006; accepted 15 March 2006

Available online 11 April 2006

**Abstract**—Holliday junctions (HJs) are formed as transient DNA intermediates during site-specific and homologous recombination. Both of these genetic exchange pathways are critical for normal DNA metabolism and repair. Trapping HJs leads to bacterial cell death by preventing proper segregation of the resulting interlinked chromosomes. Macrocyclic peptides designed to target this intermediate were synthesized with the goal of identifying compounds with specificity for this unique molecular target. We discovered ten macrocycles, both hexameric and octameric peptides, capable of trapping HJs *in vitro*. Those macrocycles containing tyrosine residues proved most effective. These data demonstrate that C-2 symmetrical macrocycles offer excellent synthetic targets for the development of novel antibiotic agents. Furthermore, the active compounds identified provide valuable tools for probing different pathways of recombinational exchange.

© 2006 Elsevier Ltd. All rights reserved.

## 1. Introduction

The emergence of new microbial pathogens coupled with a dramatic rise in the incidence of drug resistance poses a considerable challenge to human health.<sup>1–3</sup> We face the prospect of a post-antibiotic era where relatively minor hospital procedures can lead to life-threatening, untreatable infections. In order to be effective, we need new antibiotics that target unique sites in resistant strains of bacteria. The Holliday junction (HJ), a four-stranded joint (Fig. 1) derived from the recombinational exchange of DNA chains during site-specific and homologous recombination reactions,<sup>4</sup> presents a potential target for a new spectrum of antimicrobials. Recombinational processes are vital for accurate chromosomal segregation and DNA repair, the salvage of stalled replication forks, and generating the rearrangements that fuel evolution.<sup>5</sup> Blocking recombination reactions by trapping the HJ intermediate prevents transmission of

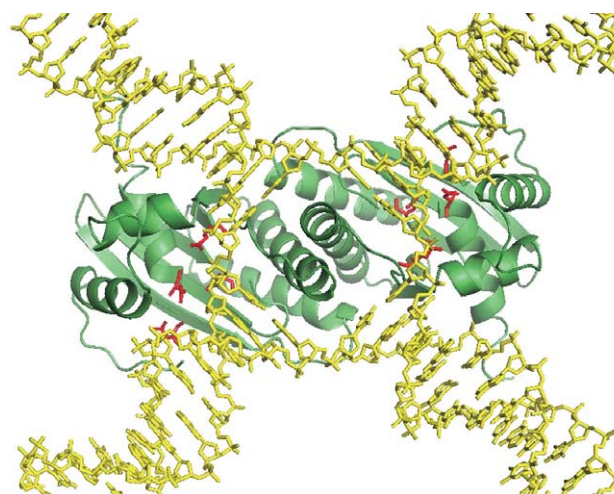


**Figure 1.** Model of *Escherichia coli* RuvC protein bound to a square planar Holliday junction. The DNA is shown in yellow and the crystal structure of homodimeric RuvC in green. Residues important for catalysis (Asp-7, Glu-66, Asp-138, and Asp-141) are highlighted in red. RuvC is thought to bind this HJ conformation during branch migration as part of a RuvABC complex.

**Keywords:** Cyclopeptides; Macrocycles; Antibiotics; Holliday junction; Antibiotic resistance; Peptides.

\* Corresponding authors. Tel.: +1 619 594 5580 (S.R.M.); e-mail: [mcalpine@sciences.sdsu.edu](mailto:mcalpine@sciences.sdsu.edu)

† These authors contributed equally to this work.

the genetic material to daughter cells leading to bacterial death. Previous studies have shown that linear dodecapeptides that successfully trap HJs in vitro also have antibacterial properties.<sup>6–8</sup> Linear peptides inhibit cell growth of Gram-positives (e.g., *Staphylococcus aureus*) in a dose-dependent manner at nanomolar concentrations. These compounds represent a new class of antibiotics reminiscent of the quinolone/fluoroquinolone group, which stabilize a normally transient intermediate.

Crystallography studies indicate that the lead linear dodecapeptides bind at the HJ center.<sup>9,10</sup> However, these leads were problematic because of their size, solubility, flexibility, and degradation within cells, making it difficult to identify specific residues involved in the binding event. In order to elucidate the biological mechanism of action, and find soluble compounds that trap this unique target, we synthesized two generations of macrocyclic peptides.

## 2. Results and discussion

Herein we describe the synthesis and biological activity of both the first generation of eight macrocyclic hexameric peptides and the second generation of eighteen hexameric and four octameric macrocyclic peptides. These macrocycles were designed to fit the C-2 symmetrical HJ binding site (approximately 25 Å by 10 Å)<sup>9</sup> and residues were chosen based on the active linear dodecapeptide leads. The four significant aspects of this work include: (i) synthetic and biological data from these unique, C-2 symmetrical class of compounds, (ii) inclusion of polar residues within the second-generation solid-phase macrocycles, (iii) the discovery that tyrosines are critical elements within the macrocycles for binding HJs, and (iv) the compounds that trap HJs offer valuable tools for dissecting recombination pathways that proceed via this intermediate. This last feature is not an option with linear dodecapeptides due to their insolubility. In addition, the macrocycles described (which are more rigid and smaller in size than the dodecapeptides) also offer the opportunity to visualize HJ–peptide interactions by X-ray crystallography, which is not possible with the linear dodecapeptides.

### 2.1. Synthesis of first generation

A first generation of C-2 symmetrical, macrocyclic, hexapeptides were synthesized using hydrophobic amino acids (Fig. 2). It was anticipated that these macrocycles would be more rigid than the linear lead peptides and their symmetry and size would not preclude their binding to the central aperture of an unfolded HJ. Aromatic residues were selected due to their presumed importance in  $\pi$ -stacking with DNA base pairs.

Our approach was chosen to simplify the synthesis of the macrocycles, while allowing easy exchange of amino acids, and incorporating residues known to trap HJs.<sup>11</sup> Using 2(1*H*-benzotriazole-1-yl)-1,1,3-tetramethyluronium tetrafluoroborate (TBTU), and diisopropylethylamine (DIPEA), acid-protected residue **1a,b** and

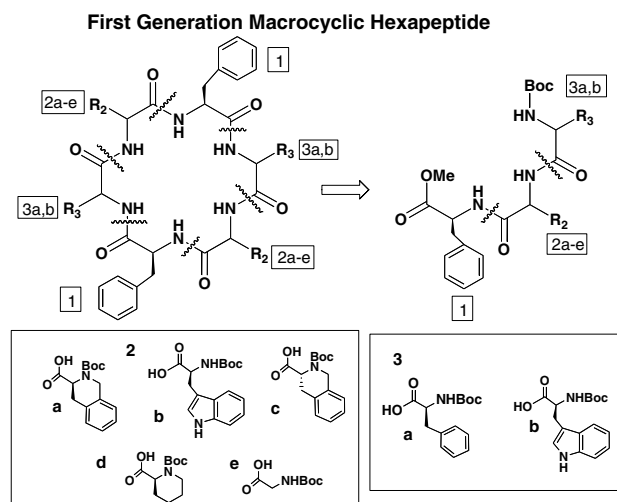


Figure 2. Monomers used in the first generation.

*N*-Boc-protected residue **2a–e** were coupled to give the dipeptide **1–2–Boc** (80–94% yield). Deprotection of the amine on residue **2** using TFA gave the free amine **1** and **2** (quantitative yields). Coupling of this dipeptide to monomer **3a,b** gave the desired tripeptide in good yields (65–94%).

The tripeptide was separated into two equal aliquots. The acid was deprotected in one aliquot using sodium hydroxide, while the amine was deprotected in the other using TFA. These two tripeptides were coupled together using multiple coupling agents, yielding eight examples of linear hexapeptides (19–73% yield). These were amine deprotected using HCl (pH < 3). Upon completion, the reaction was concentrated in vacuo, and the acid was deprotected by neutralizing the reaction with sodium hydroxide, and then adding four additional equivalents of sodium hydroxide in methanol to give pH 11. Following acid deprotection, the reaction was concentrated in vacuo and subjected to HATU, TBTU, and DEPBT coupling reagents (0.75 equiv each), and DIPEA (~6 equiv). Macrocyclizations took approximately four days due to the low concentration (0.005–0.01 M) required to maximize the yield. The final compounds were purified using reverse-phase HPLC and confirmed via LCMS.<sup>12</sup> These eight, uniquely designed, macrocyclic compounds were tested for their ability to trap HJs in vitro.

### 2.2. First-generation in vitro assays

The eight, first-generation, macrocycles were tested for their ability to trap the HJ in an in vitro site-specific recombination assay.<sup>12</sup> Three of these compounds were successful in trapping the HJ in these assays with potency similar to the linear lead Lys-Trp-Trp-Cys-Arg-Trp. Here we utilized the *Escherichia coli* RuvC protein to probe the effect of these three compounds on homologous recombination reactions in vitro. RuvC is a HJ-specific endonuclease that eliminates 4-way junctions formed by homologous recombination or replication fork regression.<sup>13</sup> RuvC (200 nM) forms a single complex with a model HJ DNA substrate (0.3 nM) labeled with <sup>32</sup>P (Fig. 3, panel 1, lane B).

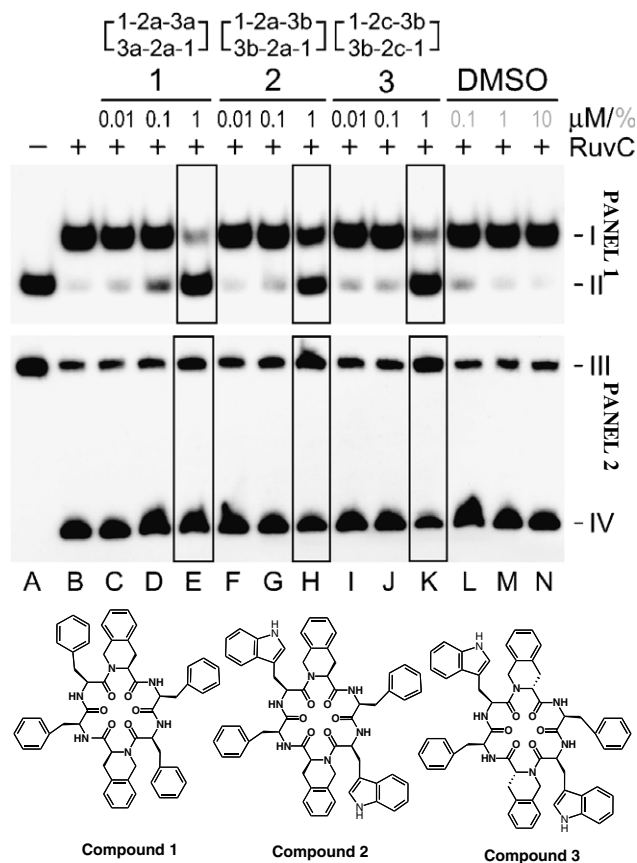


**Figure 3.** Effect of first generation compounds on RuvC binding (panel 1) I, RuvC with HJ DNA; II, peptide trapping HJ substrate. HJ resolution of  $^{32}\text{P}$ -labeled HJ DNA (panel 2) III, substrate prior to nicking; IV, nicked duplex.

At  $1\ \mu\text{M}$  the peptide trapped a significant amount of HJ substrate (panel 1, II), with the free HJ clearly accumulating in the presence of the three macrocycles (Fig. 3, lanes E, H, and K, panel I, band II) when compared to the control reaction (lane N, panel I, band I). Each of the compounds also reduced the number of complexes formed by the structurally unrelated RusA HJ resolvase<sup>13</sup> (data not shown), indicating that inhibition is due to an interaction with the junction rather than specific contacts with the resolving enzyme. These macrocycles can therefore prevent several different enzymes, including those functioning in site-specific<sup>12</sup> and homologous recombination, from gaining access to the Holliday structure. All three compounds contain phenylalanine coupled to 1,2,3,4-tetrahydroisoquinoline and it is probable that this aromatic group is involved in  $\pi$ -stacking with nucleotide bases. Furthermore, since binding assays were conducted in EDTA, the macrocycles must be binding the open square planar junction (Fig. 1) rather than the stacked-X conformation that predominates in the presence of divalent cations.<sup>14</sup>

When the experiments were repeated at  $37\ ^\circ\text{C}$  with addition of  $10\ \text{mM}\ \text{MgCl}_2$ , RuvC ( $100\ \text{nM}$ ) cleaved the HJ to generate nicked duplexes (Fig. 3, lane B, panel 2, IV). The ability to form this nicked duplex was reduced slightly by the three peptides, especially

with compound 1-2c-3b (lanes E, H, and K, compare band III to IV) as seen by the change in the proportions of substrate and product (compare band III to IV, respectively). Similar results were obtained with the linear Trp-Arg-Trp-Tyr-Cys-Arg peptide blocking HJ cleavage by RuvC.<sup>7,8,15–17</sup> The relatively poor inhibition seen with both linear and cyclic peptides may be due to a failure to bind effectively to the stacked-X conformation favored under these reaction conditions.

### 2.3. Synthesis of second generation

Hydrophobic residues, which appear in both linear and cyclic lead compounds, appear to play an important role in DNA intercalation and/or base stacking interactions at the junction cross-over. The first-generation peptides were composed entirely of hydrophobic residues, making them somewhat insoluble and unable to hydrogen-bond via side-chain residues to either DNA or proteins bound to the HJ. This may explain why the first-generation compounds succeeded at trapping HJs, but failed to show any bactericidal effect. It is also unclear how many residues participate in binding to the HJ. The first generation contained only six amino acids, but approximately six to ten amino acid residues could potentially fit into the HJ binding site. The second generation incorporated hydrophilic residues to improve solubility and hydrogen bonding properties. In addition, the testing of macrocyclic hexapeptides along with cyclic octapeptides explores an ideal ‘fit’ in the HJ.

Synthesis of eighteen, second-generation macrocycles was completed using the same conditions described for the first generation and the monomers shown in Figure 2. Interestingly, it was only when a tyrosine was included at position 7 that the cyclization of the octapeptides was successful.

### 2.4. Solution-phase second generation macrocycles

Using the same approach to that described for the first generation, the tripeptide was synthesized in good yields (65–85%). These tripeptides were converted into linear hexapeptides (13 examples, 63–94% yields) and cyclized (13 examples, 8–25% yields).<sup>11,18</sup>

The synthesis of the tetrapeptide was completed by deprotecting the tripeptide amine using TFA and coupling it to residue 7. In a similar fashion to the hexapeptides, the tetrapeptide was separated into two equal aliquots, whereupon one aliquot was acid deprotected and the other was amine deprotected. The subsequent coupling of the tetrapeptide free acid and free amine using multiple coupling agents gave four examples of linear octapeptides (36–68% yield). The octapeptides were cyclized using the same conditions as those for the macrocyclic hexapeptides, yielding four examples (18–25% yield). These final compounds were purified using reverse-phase HPLC and confirmed via LCMS.<sup>19</sup> Their ability to block formation of a RuvC–HJ complex was assayed *in vitro*.

## 2.5. Solid-phase macrocycles

For ease of synthesis with polar residues, solid phase was utilized for five hexameric macrocycles (Fig. 4). Starting with resin-bound residues **8a–c**, addition of TBTU, DIPEA, and *N*-Fmoc gave the resin-bound dipeptide 8-9-Fmoc. We coupled residue **9** a second time to ensure the reaction had gone to completion.<sup>20</sup> Deprotection of the amine on residue **9** using piperidine in DMF gave the free amine **8** and **9**. Coupling of this dipeptide to monomer **10a–c** gave the desired tripeptide in good yields (94% when cleaved).<sup>20</sup>

## 2.6. Initial solid-phase approach

Emulating the solution-phase approach, the tripeptide was separated into two equal aliquots. The acid was formed by cleaving the compound from the bead in the first aliquot using 0.5% TFA in methylene chloride. The amine was deprotected in the second aliquot using

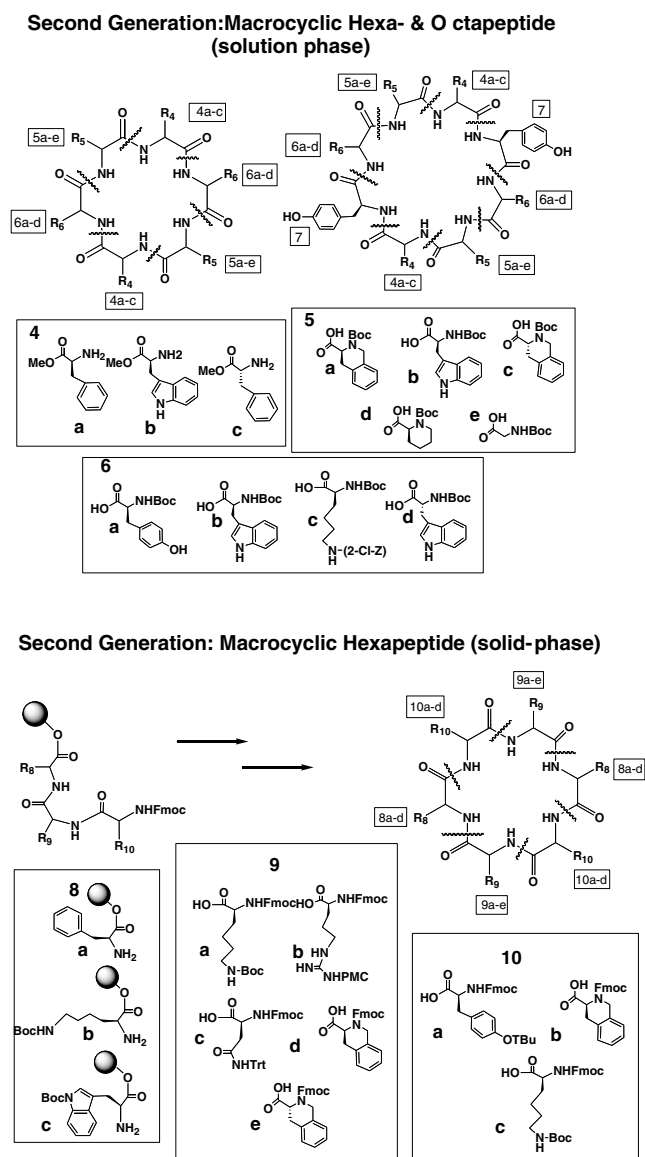


Figure 4. Monomers for solid-phase compounds.

20% piperidine in DMF. The free acid trimer, now in solution, was coupled to the resin-bound tripeptide amine. This yielded a hexapeptide bound to the resin. Subsequent amine deprotection and cleavage from the bead yielded a double deprotected linear hexamer. A purity check via LCMS revealed a very 'dirty' hexapeptide. Cyclization using our standard solution-phase conditions gave the macrocycle, but at very low yield. When analyzed, we attributed this low yield to the fact that we double coupled at all steps except when the tripeptide acid was coupled to the resin-bound amine. It was possible to perform only a single coupling of the tripeptide because of the limited free acid solution peptide cleaved from the bead.

## 2.7. Final solid-phase approach

Given the difficulties encountered using a convergent approach, we synthesized the same compound using a linear approach. The resin-bound amino acid **8a–c** was coupled to *N*-Fmoc-protected residue **9a–c**.<sup>11</sup> Double coupling of resin **9a–c** was carried out to ensure complete formation of the dimer.<sup>20</sup> Upon deprotection of the amine on residue **9**, residue **10a–c** was coupled to the dipeptide. Again double coupling was utilized to ensure complete formation of the tripeptide. Subsequent deprotection and coupling reactions were performed until the hexapeptide was formed. Cleavage of this hexapeptide to give the double deprotected linear hexamer and analysis by LCMS showed pure product.

The reaction was concentrated in vacuo and subjected to HATU, TBTU, and DEPBT coupling reagents (~1.5 equiv each), and DIPEA (~6 equiv). The final macrocyclizations took approximately four days due to the low concentration (0.005–0.01 M) required to maximize the yield. The one-pot ring-closing gave better yields (15% average) than those seen when the convergent approach was utilized (10% average). The compounds were purified using reverse phase HPLC and confirmed via LCMS. Finally, deprotection of the peptide side chains was completed using 95% TFA in methylene chloride. Five compounds were purified by HPLC and confirmed via LCMS (Fig. 6).

## 2.8. Assays of solution-phase second-generation compounds

Initially, six of the second-generation macrocycles were tested in the RuvC-junction binding assay (compounds 4–9). In RuvC–HJ binding experiments, a significant amount of HJ accumulated in the presence of all macrocycles at 1  $\mu$ M (Fig. 5 band II). Compounds 7 and 9 were particularly effective in preventing the formation of a complex between 200 nM RuvC and 0.3 nM <sup>32</sup>P-labeled HJ DNA (lanes K and O) when compared to the control without peptide (lane C). These two macrocycles appear to be at least as potent in trapping the HJ as one of the lead peptides (lane Q). It is important to note that all six compounds tested bind the HJ, and all six contain tyrosine. The presence of tyrosine appears to be critical for the HJ interaction, which is

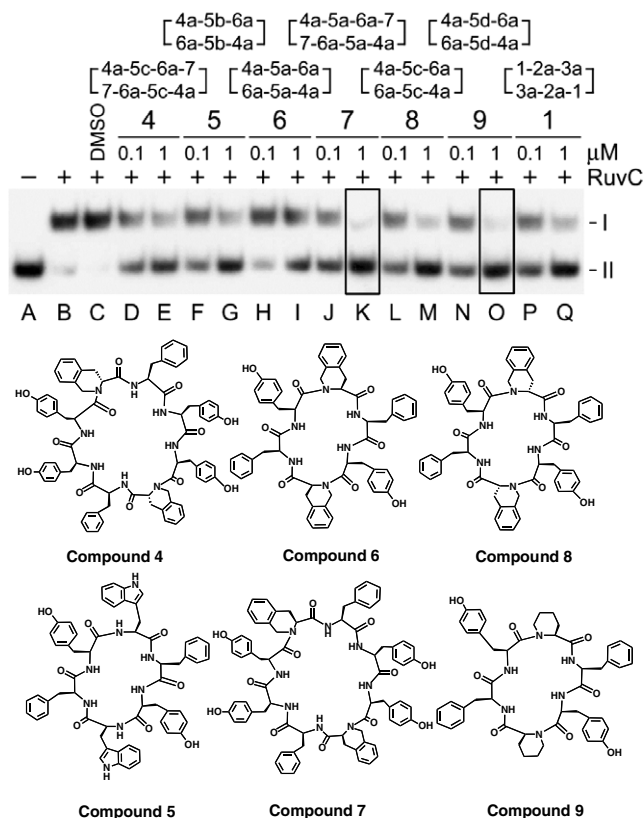


**Figure 5.** Effect of second-generation compounds on RuvC binding to <sup>32</sup>P-labeled HJ DNA. I, RuvC with HJ DNA; II, peptide trapping HJ substrate.

demonstrated not only by this data but also by the solid-phase assay data (Fig. 6).

We estimate that a hexapeptide can be readily accommodated within the central hole of a HJ in an open square planar configuration (Fig. 1). Multiple (3–4) contacts probably contribute to the stability of DNA binding and their tight association will either present a steric hindrance to protein access or restrict the ability of recombinases to fold the DNA structure correctly for catalysis. The octapeptides should also fit within the center of HJs, although clearly they will be more constrained in their mode of DNA binding. Compound 7, an octamer (Fig. 5, lane K), was more effective at blocking RuvC binding to the HJ than a structurally similar cyclic hexapeptide (lane I). Thus, the size of the peptide does not limit its trapping potential. Intercalation between nucleotide bases may be more important for these larger macrocycles, perhaps explaining the need for tyrosines, phenylalanines, and tetrahydroquinolines. Further details on these interactions require an HJ–peptide co-crystal structure. Successful binding of these compounds to HJs and determination of the important structural features required for binding is a fundamental discovery.

### 2.9. Second generation in vivo assays

In addition to the in vitro assays, growth inhibition experiments were conducted on Gram-negative (*E. coli*)

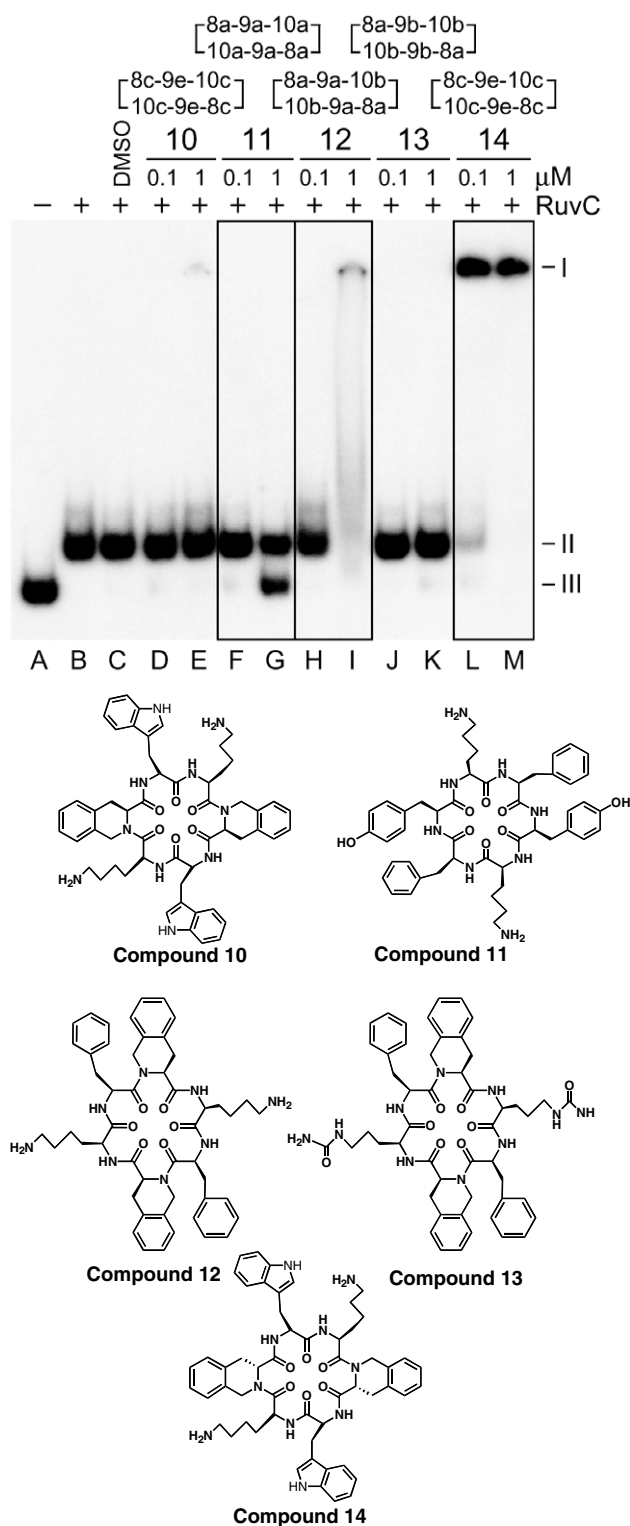


**Figure 6.** RuvC gel-shift assay of solid-phase compounds, band I, non-specific binding to DNA; II, RuvC with HJ DNA; III, peptide trapping HJ substrate.

and Gram-positive (*S. epidermidis*) bacteria. Compound 9 was tested as it was highly effective in trapping HJs. However, at 5 μM this peptide had no negative effect on the growth or survival of a wild-type *E. coli* strain (data not shown). The inability of compound 9 to inhibit bacterial growth may be in part due to its

hydrophobicity. Their hydrophobic nature may serve to limit passage across bacterial cell walls.

## 2.10. Assays of solid-phase second generation compounds

Five macrocycles (compounds **10–14**), which contained lysine or arginine, were tested for their ability to block HJs in the *in vitro* RuvC–HJ DNA binding assay. Of the five tested, one significantly reduced the ability of RuvC (200 nM) to form complexes with the radioactively labeled HJ substrate at 0.3 nM (Fig. 6, lane G, compound **11**, band III). Remarkably, this compound was the only one that contained a tyrosine, which is consistent with earlier observations of solution-phase compounds that trap HJs (Fig. 5). The incorporation of tyrosine in macrocycles for effective HJ trapping appears, therefore, to be a critical feature and may be due to tyrosine's ability to  $\pi$ -stack as well as hydrogen bond with nucleotide bases. To determine the ideal 'fit' for trapping HJs, additional experiments comparing hexapeptides versus octapeptides on HJ binding are in progress. Macrocycle **11** traps HJs, however, when tested for antibacterial activity in *E. coli* and *S. epidermidis* bacteria, no growth defect was detected (data not shown). One possible explanation for this is that compound **11** does not bind sufficient quantities of HJs to kill bacteria, or alternatively it may be unable to gain entry through the cell wall. Regardless of this issue, compound **11** provides an excellent tool for elucidating molecular pathways that involve HJ intermediates.

## 2.11. Non-specific DNA binding

In Fig. 6, peptides **12** and **14** disrupted the formation of RuvC–HJ complexes, although in this case the HJ substrate remains trapped in the wells of the polyacrylamide gel (band I, Fig. 6, lanes I and M). This may be indicative of non-specific binding with multiple peptides assembling on the DNA and preventing its entry into the gel matrix.

To confirm this possibility, the solid-phase macrocycles were examined for their ability to bind to  $^{32}\text{P}$ -labeled single-stranded (ss) and double-stranded (ds) DNA substrates (0.3 nM), in the absence of RuvC protein (Fig. 7). Compounds **10**, **11**, and **12** did not appear to bind stably to either substrate. However, compound **14** bound both ss and ds DNA, trapping all of the substrate in the well of the gel at 1  $\mu\text{M}$  (Fig. 7, lanes L and I). Compound **12** formed a much less stable association with ss and ds DNA, with at least some of the complexes being able to enter the gel (Fig. 7, lane H). These results correlate with those obtained using the HJ DNA substrate (Fig. 6).

The following conclusions for the five solid-phase compounds (**10–14**) can be drawn: (i) compounds **10** and **13** do not block RuvC binding to the HJ, which is consistent with an inability to bind at the center of the X junction; (ii) Compound **11** fails to bind unbranched DNA in Figure 7 but does block RuvC binding to HJs, indicating genuine HJ specificity. (iii) Compounds **12** and **14** bind DNA non-specifically as seen by trapping of HJ, ss

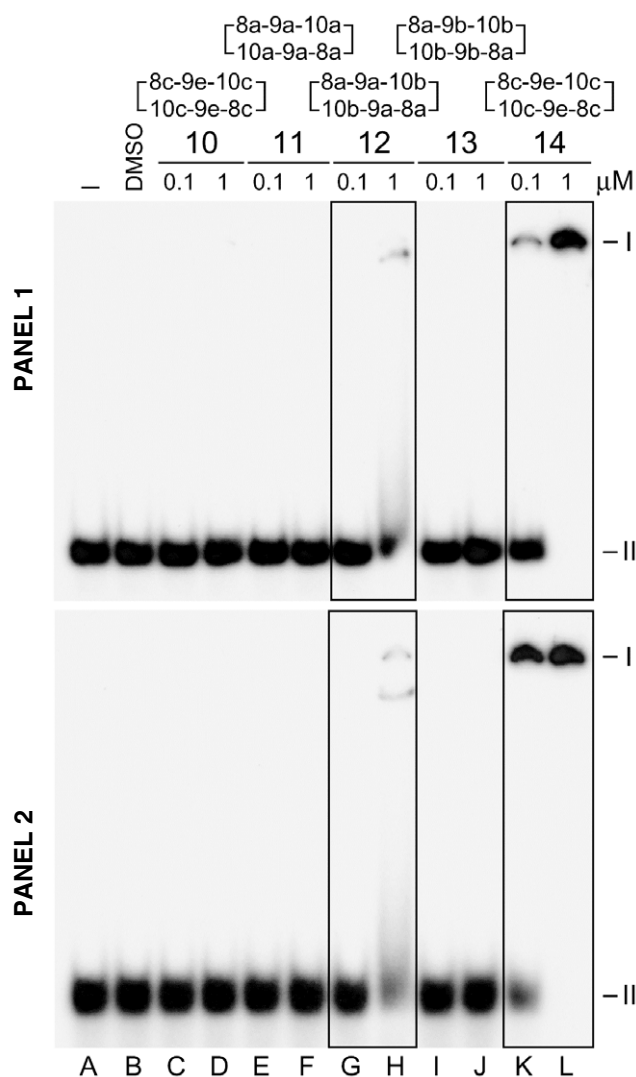


**Figure 7.** Gel-shift assay showing the binding of solid-phase compounds to  $^{32}\text{P}$ -labeled dsDNA (panel 1) I, double-stranded DNA trapped by peptide; II, double-stranded DNA not trapped by peptide. ssDNA (panel 2) I, single-stranded DNA trapped by peptide; II, single-stranded DNA not trapped by peptide.

or dsDNA at the gel origin (Figs. 6 and 7). The lack of discrimination in binding to ss or dsDNA seen with these two peptides implies that the nucleic acid interaction does not require base stacking in the helical form of B-DNA. It is unclear at this stage whether contacts are made with the phosphodiester backbone or the purine/pyrimidine bases. Clearly addition of positively charged residues can generate compounds with reduced branched DNA specificity and even closely related molecules (e.g., compounds **10** and **13**) that appear unable to interact with DNA at all. Comparison of the different properties with the structure of these compounds will assist the rational design of future macrocycles.

All five compounds were tested for antibacterial activity in *E. coli* and *S. epidermidis* bacteria. No growth defect was detected with wild-type *E. coli* (data not shown). However, two of the peptides (compound **12** and, to a significantly lesser degree, compound **14**) did inhibit

the growth of *S. epidermidis* when dilutions were spotted on a lawn of bacteria (data shown in supplementary material). Surprisingly, it was compound **12**, which forms only a relatively unstable association with ss and dsDNA that has a significant effect on bacterial growth. Further work is needed to characterize how these macrocycles interact with DNA and how this correlates with their ability to inhibit the growth of Gram-positive bacteria. In conclusion, compound **11** displays high specificity for the HJ as demonstrated by its ability to reduce the efficiency of RuvC binding to the X-structure and inability to bind unbranched DNA molecules.

### 3. Conclusions

There are four areas of significance in this described work. First, we describe the synthesis and associated biological assays on a new class of compounds. Synthesis of two generations of compounds yielded critical information that assists further development of this structural class as tools for studying pathways involving HJs during DNA repair. In addition, we have macrocycles that may lead to the development of new antibiotics. Using assays with the RuvC recombinase, we demonstrate that macrocycles successfully trap HJs *in vitro*. The second important aspect of this work is substitution of polar residues within these macrocycles. These polar residues do not play a critical role in HJ binding, but do improve compound solubility. A third, and fundamental discovery described here is the structure–activity relationship: (i) compounds containing tyrosine were highly effective at trapping HJs, and (ii) both hexapeptides and octapeptides were able to trap HJs. This discovery regarding the hexa- versus octa-peptides demonstrates that ideal fit within HJs may be reliant on the hydrophobic residues  $\pi$ -stacking with the nucleotides rather than just the macrocycle size. As the peptides bind specifically to HJs, rather than the recombinases that target HJs. We hypothesize that  $\pi$ -stacking residues, in combination with those that can also form H-bonds (e.g., tyrosine), are the key element in trapping HJs. Further work is needed to determine the precise structural requirements for trapping and antimicrobial activity. We anticipate that a third generation of macrocycles, incorporating tyrosines, hydroxy tetrahydroquinolines, and hydroxy tryptophans, will help uncover the structure–activity relationships crucial for HJ binding. Studies to determine if these compounds kill bacteria and then whether they do so via trapping HJs are on-going and will be reported in due course. Finally, perhaps the most important aspect of this work is the discovery of new macrocyclic compounds, which, by effectively trapping HJs, provide the tools for dissecting recombination pathways that proceed via this intermediate. In addition, these tools afford the opportunity to see HJ–peptide interactions via X-ray crystallography, something the linear peptides do not offer. Overall this body of work lays the foundation for further studies for this class of compounds as potential antibiotics, while providing

tools that will be utilized in mechanistic studies involving pathways with HJ intermediates.

## 4. Experimental

### 4.1. General remarks

All coupling reactions were performed under argon atmosphere with the exclusion of moisture. All reagents were used as received. Anhydrous methylene chloride Dri Solv (EM) and Anhydrous Acetonitrile Dri Solv (EM) were obtained from VWR, and were packed under nitrogen with a septum cap. Diisopropylethylamine (DIPEA) was purchased from Aldrich, packaged under nitrogen in a sure seal bottle. The coupling agent HATU and PyAOP came from Perspective: Applied Biosystems at 850 Lincoln Center Dr. Foster City, CA 94404, USA. Tel.: +1 800 327 3002 and the coupling agents TBTU and PyBROP from NovaBiochem. DEPBT [3(diethoxyphosphoryloxy)-1,2,3-benzotriazine-4(3*H*)] was purchased from Aldrich (order number 49596-4). The  $^1\text{H}$  NMR spectra were recorded on a Varian at 500 MHz. LCMS was performed at San Diego State University using HP1100 Finnigan LCQ. Flash column chromatography used 230–400 mesh 32–74  $\mu\text{m}$  60 Å silica gel from Bodman Industries.

### 4.2. General peptide synthesis in solution

All peptide coupling reactions were carried out under argon with dried solvent, using methylene chloride for dipeptide and tripeptide couplings and acetonitrile for all other peptide couplings. The amine (1.1 equiv) and acid (1 equiv) were weighed into a dry flask along with 3 equiv of DIPEA and 1.1 equiv of TBTU.<sup>‡</sup> Anhydrous methylene chloride was added for a 0.1 M solution. The solution was stirred at room temperature and reactions monitored by TLC. Reactions were run for 4–24 h before working up by washing with saturated ammonium chloride. (Note: if acetonitrile was used for the reaction, methylene chloride was added upon workup and then the resulting solution was washed with ammonium chloride.) After back extraction of aqueous layers with methylene chloride, organic layers were combined, dried over sodium sulfate, filtered, and concentrated. Flash chromatography using 0–100% ethyl acetate/hexane gave the desired peptide.

### 4.3. General amine deprotection

Amines were deprotected using 20% TFA in methylene chloride (0.1 M) with 2 equiv of anisole. The reactions were monitored by TLC, where the TLC sample was first worked up in a mini-workup using DI water and methylene chloride to remove TFA. Reactions were allowed to run for 1–2 h and then concentrated *in vacuo*.

<sup>‡</sup> Some coupling reactions failed to undergo completion using only TBTU and therefore HATU, and/or DEPBT were employed. In a few cases 1.1 equiv of all three coupling reagents were used.

#### 4.4. General acid deprotection

Acids were deprotected using 4 equiv of lithium hydroxide (or enough was added until pH ~11) in methanol (0.1 M). The peptide was placed in a flask, along with lithium hydroxide and methanol, and stirred overnight. Within 12 h the acid was usually deprotected. Work-up of reactions involved the acidification of reaction solution using HCl to pH 1. The aqueous solution was extracted three times with methylene chloride, and the combined organic layer was dried, filtered, and concentrated in vacuo.

#### 4.5. Macrocyclization procedure (in situ)

All hexa- and octa-peptides were deprotected using HCl in methanol and the presence of the free amine was verified using LCMS. The reaction was then neutralized with lithium hydroxide. Upon neutralization, LiOH was added (~4 equiv) to bring the pH up to ~11. The acid deprotection was verified via LCMS. Upon acid deprotection the reaction was concentrated in vacuo and the crude, dry, double deprotected peptide (free acid and free amine) was dissolved in a minimum of dry acetonitrile. Three coupling agents were initially used: DEPBT, HATU, and TBTU (~0.5 to 0.75 equiv each). These coupling agents were dissolved in a calculated volume of dry 50% acetonitrile and 50% methylene chloride that would give a 0.01 M solution when including the volume used for the deprotected peptide. The coupling agents were then added to the deprotected peptide solution. Three to five equivalents of DIPEA were then added to the reaction to ensure the pH was kept at or greater than 8. If the solution was not clear, DMF or methylene chloride was added but not more than 20% of the volume used for the overall reaction. Note: in some cases methylene chloride addition improved the solution clarity more than DMF, this depended on the number of methyl groups on the compound (i.e., the hydrophobicity). With at least one methyl group it was found that methylene chloride was a better solvent than DMF for clarity; with no methyl groups, DMF was the better solvent. It is important to recognize that the coupling agents are typically not very soluble in acetonitrile, which is why an additional solvent is often used.

After 24 h, TLC and LCMS (where the LCMS sample was worked up prior to injection) were taken, if no clear distinct product spot was visible, then typically PyAOP was added (0.5 equiv), and sometimes, depending on reaction clarity, 0.5 equiv of HATU were also added. The comparison for  $R_f$  value in the product spot on TLC was the protected linear hexa- or octapeptide. The reaction was allowed to run another 24 h, and checked again by TLC and LCMS. If the reaction still failed to show a clear product spot, then 0.25 equiv of DEPBT were added and the reaction continued for 24–48 h. At this point we found the reaction always demonstrated a product spot, although it was sometimes difficult to determine if it was complete (monitoring the starting material deprotected hexa- or octapeptide via LCMS was the easiest method). Upon completion, the reaction was worked up by washing

with ammonium chloride. After back extraction of aqueous layers with methylene chloride, organic layers were combined, dried over sodium sulfate, filtered, and concentrated. All macrocycles were purified using reverse phase HPLC, and a gradient of acetonitrile and DI water with 0.1% TFA.

#### 4.6. RuvC HJ binding and cleavage assays

RuvC protein was purified as described.<sup>21</sup> A synthetic 50 bp HJ substrate containing an 11 bp mobile core (J11) was labeled with <sup>32</sup>P using T4 polynucleotide kinase.<sup>22</sup> One of the HJ constituent oligonucleotides was used as a ssDNA substrate and annealed to its complementary sequence to give the dsDNA substrate. Binding assays were performed in 50 mM Tris-HCl, pH 8.0, 5 mM EDTA, 1 mM dithiothreitol, 5% glycerol, and 100 µg/ml BSA. Samples were incubated on ice for 15 min before separation on 4% PAGE in 6.7 mM Tris-HCl, pH 8.0, 3.3 mM sodium acetate, and 2 mM EDTA. HJ cleavage was assayed at 37 °C for 30 min in 50 mM Tris-HCl, pH 8.0, 1 mM dithiothreitol, 100 µg/ml BSA, and 10 mM MgCl<sub>2</sub>. Reactions (20 µl) were terminated by the addition of 5 µl of 100 mM Tris-HCl, pH 8.0, 2.5% SDS, 100 mM EDTA, and 10 mg/ml proteinase K, and incubated for a further 10 min at 37 °C. Following addition of 5 µl of loading buffer (0.25% w/v bromophenol blue, 0.25% w/v xylene cyanol, and 15% v/v Ficoll type 400), 15 µl was electrophoresed on 10% polyacrylamide gels in 90 mM Tris-borate, 2 mM EDTA. Gels were dried onto filter paper and analyzed by autoradiography.

#### 4.7. Bacterial growth inhibition assays

*Escherichia coli* K12 strains AB2463 (*recA13*) and GS1481 (*ruwC64::kan*) are derivatives of the wild-type, AB1157. *S. epidermidis* ATCC14990 was used as a wild-type strain. Bacteria were cultured in LB broth at 37 °C and growth monitored at  $A_{650\text{nm}}$ . A single 60 ml culture was grown and divided into aliquots at an  $A_{650\text{nm}}$  of 0.18. Different compounds were added at a concentration of 0.025 µM and growth monitored every 15 min. Appropriate dilutions of cultures at an  $A_{650\text{nm}}$  of 0.6 were spotted on LB agar plates and colonies counted to determine any loss in viability. Dilutions of peptides were spotted onto plates carrying a lawn of bacteria in qualitative growth inhibition experiments.

#### Acknowledgments

We thank John Rafferty (University of Sheffield, UK) for modeling RuvC bound to the Holliday structure. We are grateful to the following: Pfizer (La Jolla) for equipment and financial donations as well as their fellowships to IM (2003–2005) and CLC (SURF, Summer 2004); the SDSU McNair program for support to CLC (Summer 2003 and 2004) and IM (Summer 2004); the Howell Foundation for support for CLC (Spring 2004); and the MIRT program for travel support for IM (2003–2004) and CLC (2004). We also thank San Diego State University for additional funding. S.R.M.

was supported by NIH (AI058241-01) and FAC by BBSRC (G15625 and C514523).

### Supplementary data

Supplementary data associated with this article can be found, in the online version, at doi:10.1016/j.bmc.2006.03.028.

### References and notes

1. Neu, H. C. *Science* **1992**, *257*, 1064.
2. Shortridge, V. D.; Doern, G. V.; Brueggemann, A. B.; Beyer, J. M.; Flamm, R. K. *Clin. Infect. Dis.* **1999**, *29*, 1186–1188.
3. Kaufman, M. Worries Rise Over Effect of Antibiotics in Animal Feed. *Washington Post*, 17, March, Page A1, 2000.
4. Blakely, G.; May, G.; McCulloch, R.; Arciszewska, L. K.; Burke, M.; Lovett, S. T.; Sherratt, D. J. *Cell* **1993**, *75*, 351–361.
5. Nash, H. A. *Site-specific recombination: integration, excision, resolution, and inversion of defined DNA segments in Escherichia coli and Salmonella*; ASM: Washington, DC, 1996.
6. Although this activity could come from the peptides being dissolved in the membrane and forming channels that lead to cell lysis, we believe it is due to trapping the HJ intermediate within cells. The strain *Salmonella typhimurium* Ames, which is more permeable than the wild-type LT2 strain, is 2- to 4-fold more sensitive to the linear lead peptides than the WT LT2 strain. In addition, peptide addition during dividing cells (mid-log phase of growth) blocked further growth but did not cause decreases in turbidity, which suggests that lysis is not occurring. Finally, C-terminus rhodamine-labeled peptides retain inhibitory activity, thus peptide transport is not a concern.
7. Klemm, M.; Cheng, C.; Cassell, G.; Shuman, S.; Segall, A. M. *J. Mol. Biol.* **2000**, *299*, 1203–1216.
8. Cassell, G.; Klemm, M.; Pinilla, C.; Segall, A. M. *J. Mol. Biol.* **2000**, *299*, 1193–1202.
9. Gopaul, D. N.; Guo, F.; VanDuyne, G. D. *EMBO J.* **1998**, *17*, 4175–4187.
10. Unpublished results from Gunderson/Segall Lab.
11. See [Supplementary data](#) for scheme and details.
12. Bolla, M. L.; Azevedo, E. V.; Smith, J. M.; Taylor, R. E.; Ranjit, D. K.; Segall, A. M.; McAlpine, S. R. *Org. Lett.* **2003**, *5*, 109–112.
13. Sharples, G. J. *Mol. Microbiol.* **2001**, *39*, 823–834.
14. Duckett, D. R.; Murchie, A. H.; Diekmann, S.; Kitzing, E. V.; Kemper, B.; Lilley, D. M. *Cell* **1988**, *55*, 79–89.
15. Boldt, J. L.; Pinilla, C.; Segall, A. M. *J. Biol. Chem.* **2004**, *279*, 3472–3483.
16. Ghosh, K.; Lau, C. K.; Guo, F.; Segall, A. M.; VanDuyne, G. D. *J. Biol. Chem.* **2005**, *280*, 8290–8299.
17. Kepple, K. V.; Boldt, J. L.; Segall, A. M. *Proc. Natl. Acad. Sci. USA* **2005**, *102*, 6867–6872.
18. Hexa peptide macrocycles synthesized: (1) 4 = a, 5 = a, 6 = a, (2) 4 = a, 5 = b, 6 = a, (3) 4 = a, 5 = c, 6 = a, (4) 4 = a, 5 = d, 6 = a, (5) 4 = a, 5 = e, 6 = a, (6) 4 = b, 5 = a, 6 = a, (7) 4 = a, 5 = a, 6 = c, (8) 4 = b, 5 = a, 6 = c, (9) 4 = b, 5 = c, 6 = c, (10) 4 = a, 5 = c, 6 = c, (11) 4 = b, 5 = c, 6 = a, (12) 4 = c, 5 = a, 6 = d, (13) 4 = c, 5 = c, 6 = d, octapeptide macrocycles synthesized (1) 4 = a, 5 = a, 6 = a, 7 (2) 4 = a, 5 = b, 6 = a, 7 (3) 4 = a, 5 = c, 6 = a, 7 (4) 4 = a, 5 = d, 6 = a, 7.
19. Liotta, L. A.; Medina, I.; Robinson, J. L.; Carroll, C. L.; Pan, P.-S.; Corral, R.; Johnston, J. V. C.; Cook, K. M.; Curtis, F. A.; Sharples, G. J.; McAlpine, S. R. *Tetrahedron Lett.* **2004**, *45*, 8447–8450.
20. Ninhydrin tests typically demonstrated a very light blue color after coupling. Upon a second coupling they gave yellow beads.
21. Dunderdale, H. J.; Sharples, G. J.; G., L. R.; C., W. S. *J. Biol. Chem.* **1994**, *269*, 5187–5194.
22. Sharples, G. J.; Curtis, F. A.; McGlynn, P.; Bolt, E. L. *J. Mol. Biol.* **2004**, *340*, 739–751.